

## ARTICLE

# A Measurement Method for Cesium Contamination Distribution on the Bottom of a Top Shield Plug from the Operation Floor of the Fukushima Daiichi Nuclear Power Plant

Ikuo KANNO\*, Keisuke OKUMURA, Taichi MATSUMURA, Eka Sapta RIYANA, Kenichi TERASHIMA and Masahiro SAKAMOTO

*Collaborative Laboratories for Advanced Decommissioning Science (CLADS),  
Japan Atomic Energy Agency, Tomioka, Fukushima, 979-1151, Japan*

For the decommissioning of the Fukushima Daiichi Nuclear Power Plant, Cs-137 contamination distribution on the bottom of a top shield plug must be estimated. Gamma rays emitted from the surface of an operation floor and inner walls of a reactor building, however, disturb the contamination distribution measurement. This paper proposes a direct measurement method of Cs-137 contamination distribution on the other side of a concrete shield plug with a gamma ray pinhole camera based on deterministic calculations.

**KEYWORDS:** nuclear power plant accident, decommissioning, Cs-137 contamination, direct measurement, gamma ray pinhole camera

## I. Introduction

In the accident of the Fukushima Daiichi Nuclear Power Plant (1F) induced by a great Tsunami in March 2011, radioactive Cs isotopes were released from the primary containment vessel (PCV). Above the PCV, three layers (top, middle, lower) of shield plugs made of concrete were placed as shown in Ref. 1). The thickness of each shield plug was nearly 60 cm, and the diameter of the top shield plug was 1200 cm. Each shield plug consisted of three parts: left, center and right lids with gaps between them. The gap directions of three-layer shield plugs changed 90 degrees alternatively. However, Cs isotopes passed through the gaps and contaminated the surfaces of shield plugs and walls of a reactor building.

After 13 years from the accident, the remaining Cs isotopes is Cs-137. The amount of Cs-137 contamination at the bottom of the top shield plug is under study for the preparation of decommissioning. The upper surface of the top shield plug is called an operation floor, where operators can perform maintenance works. Dose rate measurement on the operation floor is not suitable for the estimation of Cs-137 contamination on the bottom of the top shield plug: the operation floor surface itself is also contaminated and the gamma rays from the building walls disturb the measurement.

To overcome this difficulty, a measurement method was invented with an assumption of uniform Cs-137 contamination distributions on the operation floor surface and on the bottom of the top shield plug: dose rate measurements as a function of depth of a dose rate meter in holes bored on

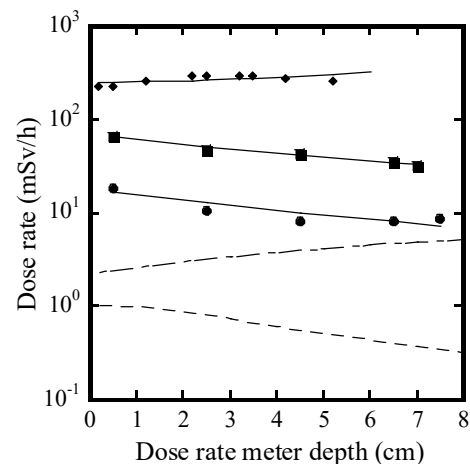


**Fig. 1** Dose rate as a function of the depth of dose rate meter depth. Dashed and dash-dot lines show the contributions of uniform contamination distributions on the operation floor surface and on the bottom of the top shield plug with  $10^5$  and  $10^9$  Bqcm<sup>-2</sup>. Symbols are measured dose rates at No. 2 (circles), No.3 (squares) and IRID-east (diamonds) holes<sup>1)</sup>. Solid lines are fitted results by the linear combinations of dashed and dash-dot lines.

the operation floor<sup>1)</sup>. **Figure 1** shows the effects of contaminations on the operation floor surface (dashed line) and on the bottom of the top shield plug (dash-dot line) with the uniform contamination densities of  $10^5$  and  $10^9$  Bqcm<sup>-2</sup>, respectively, behaving in opposite ways: when the dose rate meter is placed deep in the hole, it is away from the operation floor surface and also close to the bottom of the top shield plug. The measured dose rates in some of the bored holes

\*Corresponding author, E-mail: ikuo.kanno@gmail.com

shown in Ref. 1) are also plotted in Fig. 1. With fitting the measured dose rate change as a function of the dose rate meter depth, the amount of uniform contaminations on the operation floor surface and on the bottom of the top shield plug can be estimated.

The estimated contamination density on the bottom of the top shield plug and the one on the operation floor surface, however, ranged from  $4 \times 10^8 \sim 6 \times 10^{11}$  and  $2 \times 10^5 \sim 4 \times 10^6$  Bq  $\text{cm}^{-2}$ , according to the positions of the holes. Also, dose rate measurements on the operation floor by a detector shielded by thick lead showed non-uniform distribution. These measurements showed the uniform contamination assumption was not appropriate.

In this paper, we propose a method for a direct measurement of Cs-137 contamination distribution on the bottom of the top shield plug. For this purpose, a gamma ray pinhole camera is employed. First, details on the pinhole camera are described. An application method of the pinhole camera for the measurement of Cs-137 contamination distribution on the other side of the concrete shield plug is followed. Finally, a planned experiment for the feasibility study of this method is proposed.

## II. Gamma Ray Pinhole Camera

A gamma ray pinhole camera consists of a gamma ray shield with a pinhole and a two-dimensional pixel detector.<sup>2)</sup> The gamma rays passed through the pinhole are detected and imaged: the detection efficiency of the pinhole camera is low. On the other hand, it has an advantage that the pixel position corresponds to the direction of gamma ray incidence.

For the improvement of the detection efficiency, a coded aperture camera was developed, which had many holes for gamma rays to pass.<sup>3)</sup> The coded aperture camera has a disadvantage that the incident direction of gamma rays is not related to a pixel position directly. Also, the analysis method of measured data is complicated.

The one-by-one relationship between the gamma ray incidence direction and the pixel position of the pinhole camera is a great advantage for our application. Even though the gamma ray shield is heavy and the detection efficiency is low, compared to a Compton camera<sup>4)</sup>, the pinhole cameras are employed for contamination measurements widely.

In general, gamma cameras described above observe gamma ray sources, i.e., radioactive contaminations, with the assumption that they are on the surfaces which are visible from optical cameras attached to them. Exceptional trial to find a radioactive source which is not seen from the optical camera is the one performed by Sato<sup>5)</sup> to detect Cs-137 source on the other side of a cardboard box.

For the feasibility study of Cs-137 contamination distribution measurement on the other side of the concrete shield plug with the pinhole camera by calculation, the specification of the pinhole camera was taken from the one developed by Ueno, Hitachi, Ltd.<sup>6)</sup>: the diameter of the pinhole is 6 mm, and at 5 cm from the pinhole a CdTe pixel detector with  $4 \times 4$  cm ( $16 \times 16$  pixels) is placed.

## III. Geometry for Cs-137 Contamination Measurement

For the simplicity of calculation, a 4 cm long line sensor with 17 sensors 0.25 cm apart is used in this paper, instead of the  $4 \times 4$  cm pixel detector. The center of 4 cm line sensor is defined as  $x = 0$ . **Figure 2** shows the gamma rays emitted by the contaminations on the bottom of the top shield plug and on the operation floor surface and entering the line sensor.

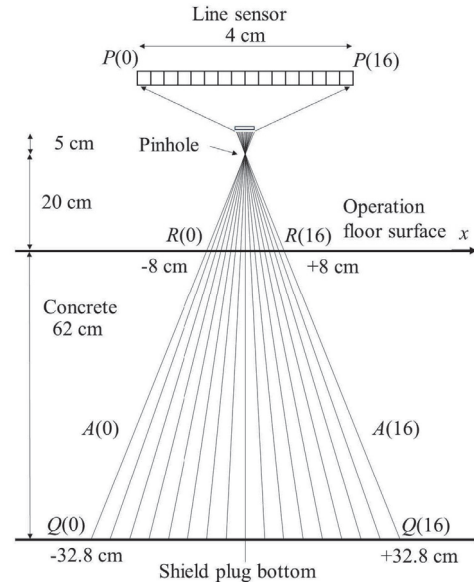


**Fig. 2** Gamma rays emitted by contaminations on the bottom of the top shield plug  $Q(j)$  and on the operation floor  $R(j)$  and observed by the pinhole camera with a 4 cm long line sensor placed 20 cm above the operation floor surface are shown by solid lines. The attenuation factors for the gamma rays emitted by  $Q(j)$  are assigned  $A(j)$ . The pixel values are shown by  $P(j)$ .

The line sensor is placed 20 cm above the operation floor surface. When the thickness of the concrete shield plug is 62 cm, the gamma rays emitted by the contamination on the shield plug bottom in the range from -32.8 to +32.8 cm are measured by the line sensor. Also, the gamma rays emitted from the contamination on the operation floor surface in the range from -8 to +8 cm are entering into the line sensor. Here,

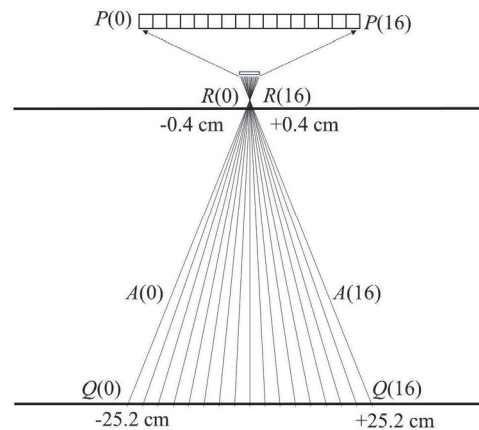


**Fig. 3** The same with Fig. 2 but the pinhole camera is placed 1 cm above the operation floor surface.

we assign the contamination densities on the shield plug bottom and on the operation floor surface as  $Q(0)$  to  $Q(16)$  and  $R(0)$  to  $R(16)$ , respectively.

The gamma rays emitted from the shield plug bottom are attenuated by the concrete. The degree of attenuation, i.e., attenuation factor, is calculated according to the Lambert-Beer law<sup>7)</sup> as a function of the path length of gamma rays inside the concrete and is assigned as  $A(0)$  to  $A(16)$ .

The number of gamma rays entering into the line sensor,  $P(j)$ , is written as follows,

$$P(j) = Q(16-j)A(16-j) + R(16-j). \quad (j = 0,16) \quad (1)$$

Here,  $P(j)$  is the measured value and  $A(j)$  is the calculated one. Estimating  $Q(j)$  and  $R(j)$  simultaneously is, however, not very easy, even though a kind of maximum likelihood method is employed.

With bringing the pinhole camera closer to the operation floor surface at 1 cm as shown in Fig. 3, the contamination ranges change from -25.2 to +25.2 cm on the shield plug bottom and from -0.4 to +0.4 cm on the operation floor surface.

With assuming the contamination density in 0.8 cm width uniform, Eq. (1) can be rewritten,

$$P(j) = Q(16-j)A(16-j) + R, \quad (j = 0,16) \quad (2)$$

where  $R$  is a constant.

Furthermore, the pinhole camera position on the operation floor surface can be moved so that  $Q(j)$  is observed at two pinhole camera positions as shown in Fig. 4. Here, the pinhole camera positions are changed as positions 0, 1 and 2 to show the principle of the measurements. The contamination densities on the shield plug bottom are defined from  $Q(0)$  to  $Q(32)$ .

The number of gamma rays measured by the pinhole camera position  $i$  ( $i=0, 2$ ) and the sensor number  $j$  ( $j=0, 16$ ) is written,

$$P(i,j) = Q(8i + 16 - j)A(16 - j) + R(i). \quad (i = 0,2, j = 0,16) \quad (3)$$

The contamination densities,  $R(i)$ , on the operation floor surface at the camera positions  $i$  ( $i=0, 2$ ), are defined as 1

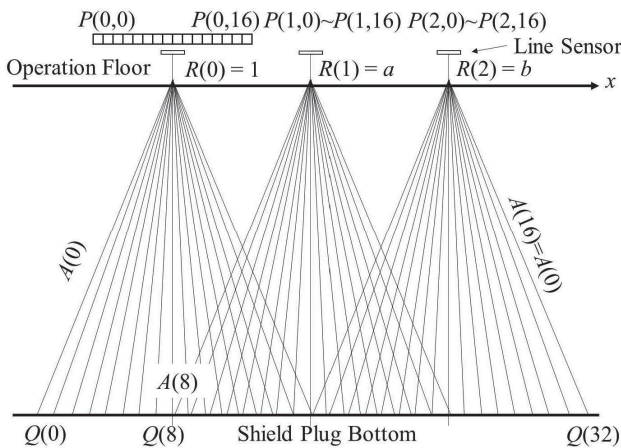


Fig.4 Change of the pinhole camera positions for observing the contamination densities at two camera positions.

(normalizing point),  $a$  and  $b$ .

#### IV. Contamination Density Estimation Method

For example, contamination density  $Q(8)$  is estimated in this section. The pixel values of the line sensor measuring the gamma rays emitted by  $Q(8)$  are  $P(0,8)$  and  $P(1,16)$ . These pixel values are written as follows,

$$P(0,8) = Q(8)A(8) + 1, P(1,16) = Q(8)A(0) + a. \quad (4)$$

Here,  $P(0,8)$ ,  $P(1,16)$  are measured values and  $A(0)$ ,  $A(8)$  are estimated ones. Unknowns are  $Q(8)$  and  $a$ . With two equations, these unknowns can be calculated.

We defined a contamination density distribution on the bottom of the top shield plug arbitrary as shown in Fig. 5. The contamination density ranges from  $10^4$  to  $5 \times 10^6$  times greater than the normalized value on the operation floor surface. Also, the contamination densities on the operation floor at the camera positions 1 and 2, i. e.,  $a$  and  $b$ , were assigned as 2 and 3, respectively.

The obtained pixel values at the pinhole camera positions 0, 1, 2 are also shown in Fig. 5 by rectangles, diamonds and triangles for  $P(0,j)$ ,  $P(1,j)$  and  $P(2,j)$ , respectively.

For the sensitivity estimation of measured pixel values, 20% of error is assumed for  $P(0,8)$  value as shown by an error bar. The values of  $Q(8)$  which correspond to both the upper and lower  $P(0,8)$  values were calculated by Eq. (4) and are shown by the error bar on  $Q(8)$ . The 20% of measurement error does not affect much on the result of the contamination ratio.

In the same way, the contamination density on the operation floor surface at camera position 1, i.e.,  $a$ , was estimated with assuming the 20% of errors for both  $P(0,8)$  and  $P(1,16)$  with Eq. (4). With the combinations of minimum and maximum values and the values without errors of  $P(0,8)$  and  $P(1,16)$ , the constant  $a$  varied from 0.21 to 3.8. The averaged

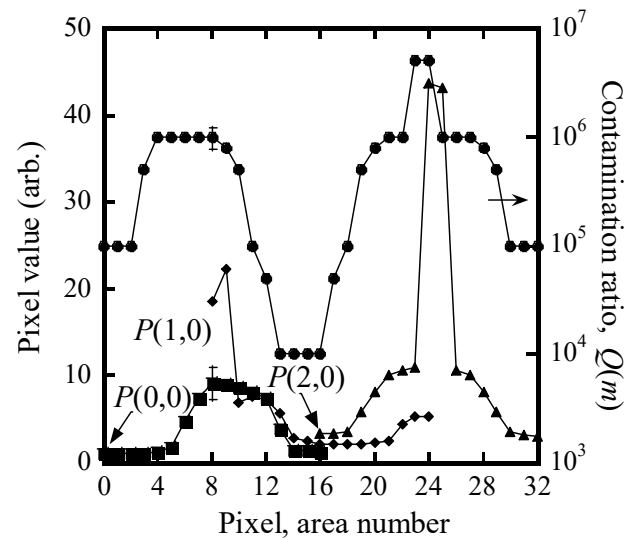


Fig. 5 Hypothetical contamination ratio distribution on the bottom of the top shield plug (circles) and pixel values of line sensor with pinhole camera positions 0 (squares), 1 (diamonds) and 2 (triangles). Assumed measurement error of 20% shown in  $P(0,8)$  is reflected on  $Q(8)$ .

value for 9 combinations of  $P(0,8)$  and  $P(1,16)$ , however, was 2, exactly. We think this is the advantage of multiple measurements for the contamination density on the shield plug bottom: we will not know whether the measured values are smaller or greater than the ones without error, and the constants  $a$  and  $b$  can be given by the average values for 17 measurements, which should be reasonable ones.

## V. Feasibility Demonstration Experiment

Before applying the method described above into practice, we are planning a feasibility demonstration experiment with Cs-137 radioisotopes in a laboratory. The available Cs-137 radioisotopes have limitations in intensities, from 1 kBq to 1 MBq. On the other hand, 60 cm thick concrete attenuates the intensity of gamma rays to less than  $10^{-5}$ . This is why the contamination density on the bottom of the top shield plug was assumed four orders of magnitude greater than the one on the operation floor surface in Fig. 5.

A proposed experimental setup is shown in Fig. 6. Instead

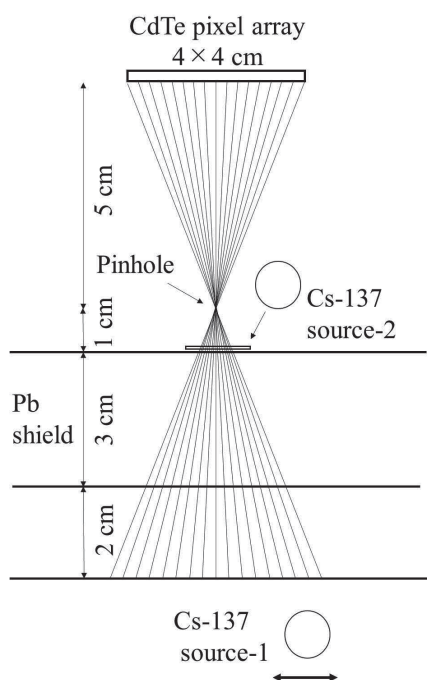


**Fig. 6** Planned experimental setup for the feasibility demonstration of the proposed measurement method for the contamination distribution on the other side of the concrete shield plug.

of 60 cm thick concrete, 3 cm thick lead is used as a substitute for the shield plug. A Cs-137 source-1 with the intensity of 1 MBq is placed 2 cm below the bottom of the lead shield, which is a hypothetical surface of the simulated bottom of the top shield plug. The pinhole camera is placed at 1 cm above the surface of the lead shield. The 4.0×4.0 cm CdTe pixel

detector observes 4.8×4.8 cm area of the hypothetical surface of the bottom of the top shield plug. The Cs-137 source-1 should be placed with changing positions on the hypothetical surface for the gamma ray detection by each CdTe pixel. With placing lead sheets with the thicknesses of 0.5 or 1.0 mm on the Cs-137 source-1, the intensity of emitted gamma rays, i.e., contamination density, can be changed for simulating a non-uniform contamination distribution. Another Cs-137 source-2 with its intensity 1 kBq is placed on the top surface of the lead shield as a simulated contamination on the operation floor surface.

## VI. Conclusion

For planning the decommission of 1F, it is important to know the Cs-137 contamination distribution on the bottom of the top shield plug. In this paper, a novel measurement method is proposed to estimate the contamination distribution on the other side of a thick concrete shield directly with using a gamma ray pinhole camera. A feasibility demonstration experiment is also proposed. With applying this method, the intensity of contamination behind an object with known thickness can be estimated.

## Acknowledgement

The authors are grateful to Dr. Y. Sato, Japan Atomic Energy Agency, for the discussions on the usage of gamma ray imagers.

## References

- 1) H. Hirayama, K. Iwanaga, K. Hayashi, K. Kondo, S. Suzuki, Z. Yoshida, "Estimated  $^{137}\text{Cs}$  radioactivity in the gap between the top and middle covers at a shield plug in the Fukushima Daiichi Nuclear Power Station Unit 2," *Nucl. Sci. Eng.*, **198**, 228-244 (2024).
- 2) C-H. Baek, S. J. An, H-I. Kim, S. W. Kwak, Y. H. Chung, "Development of a pinhole gamma camera for environmental monitoring," *Rad. Meas.*, **59**, 114-118 (2013).
- 3) M. J. Cieřlak, K. A. Gamage, R. Glover, "Coded-aperture imaging systems: Past, present and future development-A review," *Rad. Meas.*, **92**, 59-71 (2016).
- 4) R. K. Parajuli, M. Sakai, R. Parajuli, M. Tashiro, "Development and applications of Compton camera-A review," *Sensors*, **22**, 7374 (2022).
- 5) Y. Sato, "Identification of depth location of a radiation source by measurement from only one direction using a Compton camera," *Appl. Rad. Isot.*, **195**, 110739 (2023).
- 6) Y. Ueno, I. Takahashi, T. Ishitsu, et al., "Development of a high sensitivity pinhole type gamma camera using semiconductors for low dose rate fields," *Nucl. Instrum. Method in Phys. Res.*, **A893**, 15-25 (2018).
- 7) J. Hsieh, "Computed tomography," 2nd ed. Washington: SPIE Press (2009).